Polymer Bulletin 45, 183-190 (2000)

Polymer Bulletin


# Effects of acrylonitrile content on the properties of clay-dispersed poly(styrene-*co*-acrylonitrile) copolymer nanocomposite

**Moon Bae Ko**

Material Science and Technology Division, Korea Institute of Science and Technology, Seoul 130-650, Korea

Received: 1 May 2000/Revised version: 10 July 2000/Accepted: 24 July 2000

## Summary

Clay-dispersed nanocomposites have been prepared by simple melt-mixing of two components, i.e. poly(styrene-*co*-acrylonitrile) copolymers with different contents of acrylonitrile comonomer and two different kinds of organophilic clay (Cloisite® 25A and Cloisite® 30A), with a twin screw extruder. Dispersion behavior of 10-Å-thick silicate layers of clay in the nanocomposites was investigated by using an X-ray diffractometer and a transmission electron microscope. It was found that acrylonitrile comonomer incorporated into poly(styrene-*co*-acrylonitrile) copolymers accelerates intercalation of the copolymers into the galleries of silicate layers modified with an organic intercalant. The faster intercalation of a matrix polymer leads to the better dispersion of silicate layers in the matrix polymer.

## Introduction

Dispersion of smectite clays and other layered inorganic materials that can be broken down into nano-scale building blocks in polymer matrix is a good method for the preparation of organic-inorganic nanocomposites. While nanocomposites can be made in a number of ways, this paper will report on studies of melt blending the clay into the polymer. Inorganic montmorillonite surface is modified by organic treatments to make the platelet more compatible with an organic polymer. It is well documentated that the choice of organic treatment influences the degree of dispersion of the montmorillonite in the polymer matrix (1-3). Also, this paper will show that the comonomer incorporated into a matrix polymer can significantly influence the degree of dispersion in melt blending process. Figure 1 is a schematic diagram showing the situation that a polymer chain intercalates into a gallery between two silicate layers. It is expected that a large entropy loss takes place when a polymer chain in melt with a radius of gyration about a few tens of nanometer intercalates into a narrow gallery with a thickness of about 1 nm. There must be a strong interaction between polymer chain and the surface of silicate layer (and/or intercalant) in order for a long polymer chain to

Tel) +82-2-958-5335, Fax) +82-2-958-5309
E-mail) mbko@kistmail.kist.re.kr

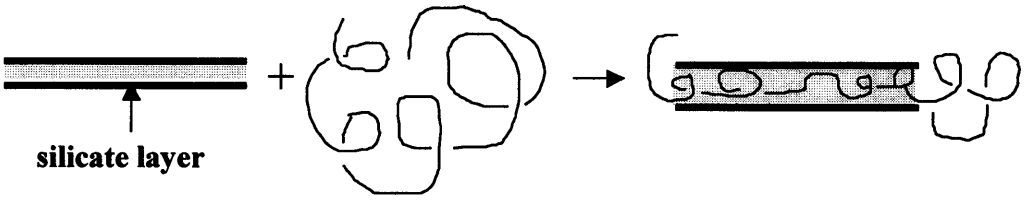


**Figure 1.** A schematic diagram showing the situation that a polymer chain intercalates into a gallery between two silicate layers. The shaded area represents the organic intercalant molecules.

intercalate into a narrow gallery of silicate layers. Therefore the selection of intercalants and functional groups in a polymer chain plays a crucial role in accelerating the intercalation of a polymer chain with smaller strength of interaction with the surface of silicate layer, such as polystyrene.

In the present work, clay/poly(styrene-*co*-acrylonitrile) copolymer (SAN) hybrids have been prepared by simple melt-mixing of two components with a twin screw extruder. Four kinds of matrix polymers with different contents of acrylonitrile comonomer were used in order to compare the effects of the content of functional group on the degree of dispersion of silicate layers of clay. Also, two different kinds of organophilic clays were used in order to compare the effects of interaction between intercalants and matrix polymers on the degree of dispersion of silicate layers. Dispersion behavior of 10-Å-thick silicate layers in the hybrids was investigated by using a transmission electron microscope and an X-ray diffractometer.

## Experimental

*Materials*. "Cloisite®" supplied by the Southern Clay Products Inc. is a trade name of organophilic clays. Two kinds of intercalants were used in the study: dimethyl hydrogenated-tallow (2-ethylhexyl) ammonium (2MHTL8, Cloisite® 25A) and methyl tallow bis-2hydroxyethyl ammonium (MT-2EthOH, Cloisite® 30A). It is noteworthy that a molecule of MT-2EthOH contains two hydroxyl groups so that it is expected that nitrile groups of SAN can interact specifically with the intercalant through hydrogen bonding. The chemical structures of intercalants are depicted in Figure 2, where HT is predominantly an octadecyl chain (C18) with smaller amounts of lower homologues (approximate composition: ~65% C18, ~30% C16, ~5% C14). Its inorganic content was calculated by measuring the weights before and after burning its organic parts. The basal spacing of organophilic clay was measured by an X-ray diffraction method. The characteristic properties of organophilic clays are summarized in Table I. Polystyrene (PS) and SAN copolymers with three different contents of acrylonitrile comonomer (5 wt.%, 25 wt.%, and 41 wt.%) were obtained from Cheil Industries Inc. Size-exclusion chromatography (SEC) analysis of polymers was performed at a flow rate of 1.0 mL/min in THF at 30 °C using a Water HPLC component system equipped with five Ultra–styragel® columns (2 x $10^5$, $10^4$, $10^3$, 500 Å) after calibration with standard polystyrene samples. The measured molecular weights are listed in Table II. *Preparation of Hybrids*. The powdery organophilic clay and matrix polymer were dry-mixed. The mixture was melt-blended by using a twin screw extruder (Model TSE 16TC, Prism) at 180 °C to yield pale-yellow strand of hybrid. The obtained strands

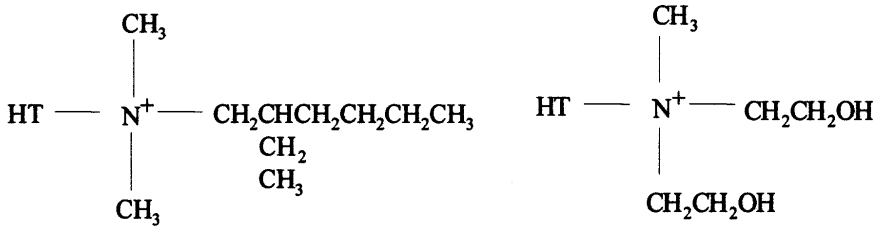


**Figure 2.** Chemical structures of two kinds of intercalants used in this study.

Table I. Charateristic properties of the organophilic clays used in this study

| Code | Organic Modifier | Modifier Concentration (meq/100g) | Weight Loss on Ignition (%) | *d*-spacing (Å) |
|---|---|---|---|---|
| Cloisite® 25A | 2MHTL8 | 95 | 34 | 20.0 |
| Cloisite® 30A | MT-2EthOH | 95 | 32 | 18.2 |

Table II. Molecular weight of poly(styrene-*co*-acrylonitrile) copolymers

| Code | PS | SAN5 | SAN25 | SAN41 |
|---|---|---|---|---|
| $M_n$ ($x10^3$) | 104 | 90 | 56 | 55 |
| $M_w$ ($x10^3$) | 242 | 304 | 109 | 106 |

were chopped with a pelletizer, and were extruded again. For this study the inorganic content in a hybrid was fixed at 5 wt.%.

*Evaluation of the Degree of Dispersion of Clay.* The degree of dispersion of silicate layers in the hybrid was evaluated by using an X-ray diffractometer and a transmission electron microscope (TEM). An X-ray diffractometer (Model MXP18, MacScience) was adopted to monitor the change in *d*-spacing of montmorillonite after intercalation. CuK$\alpha$ ($\lambda$ = 1.54 Å) was used as X-ray source at a generator voltage of 40 kV and current of 100 mA. The basal spacing of silicate layers, *d*, was calculated using the Bragg's law, $\lambda=2d\sin\theta$ from the position of (001) plane peak in XRD pattern. TEM (Model CN30, Philips) observations of the hybrids were performed for injection-molded samples, and were operated at an acceleration voltage of 120 kV. Thin sections of 70 nm were microtomed with a diamond knife and then subjected to TEM observation without staining.

*Measuring the Mechanical Properties of Hybrids.* Flexural tests of hybrids were carried out with an Instron Model 4201 at room temperature. The crosshead speed was 1 mm/min. All measurements were performed for five replicates of rectangular specimens, which were injection-molded with a Mini-Max molder, and the reported value is the mean value of those five measurements.

**Results and discussion**

Figure 3 shows XRD patterns of the clay nanocomposites melt-mixed with the twin

screw extruder. The (001) plane peaks are observed around 2.5° ~ 3.0° in XRD patterns of the hybrids except for PS/Cloisite® 30A hybrid. Therefore it can be said that intercalation of polymer chains into the galleries of silicate layers take place. However, any (001) plane peak is not observed around 2.5° ~ 3.0° in the XRD pattern of PS/Cloisite® 30A hybrid. Thus it might be, at a glance, conjectured that most of silicate layers lose their crystallographic ordering in the hybrid and the exfoliation of organophilic clay occurs. Also, it is noteworthy that the intensity of (001) plane peak from PS/Cloisite® 25A hybrid is much smaller.

Figure 4 shows TEM micrographs for the various hybrids. Clay particles (*or* so-called primary particles) are distributed in PS/Cloisite® 25A hybrid, though they are bigger than those found in SAN5/clay hybrids. However, it is observed that clay agglomerates in $\mu$m-size are distributed in PS/Cloisite® 30A hybrid, instead of clay particles or nano-scale building blocks found in any other hybrids. Hydroxyl groups of MT-2EthOH can form stable hydrogen bondings in the galleries of Cloisite® 30A because they act as proton donor/acceptor. Non-hydrogen bonding liquid such as polystyrene does not compatible with MT-2EthOH because the interaction between proton of MT-2EthOH and non-hydrogen bonding liquid makes a positive contribution to exchange energy of mixing (4). Therefore polystyrene does not intercalate into the galleries of Cloisite® 30A, resulting in no observation of (001) plane peak around 2.5° ~ 3.0° in the XRD pattern of Figure 3, and thus clay agglomerates does not break into the nano-scale building blocks. Meanwhile, the presence of 2MHTL8 in the galleries of Cloisite® 25A renders the hydrophilic silicate layer more organophilic so that

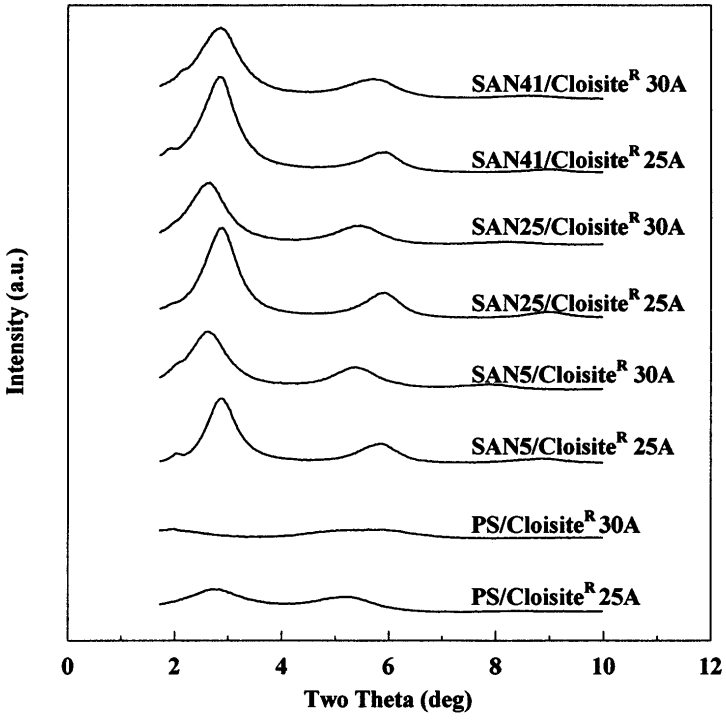


**Figure 3.** XRD patterns of the clay composites melt-mixed with the twin screw extruder.

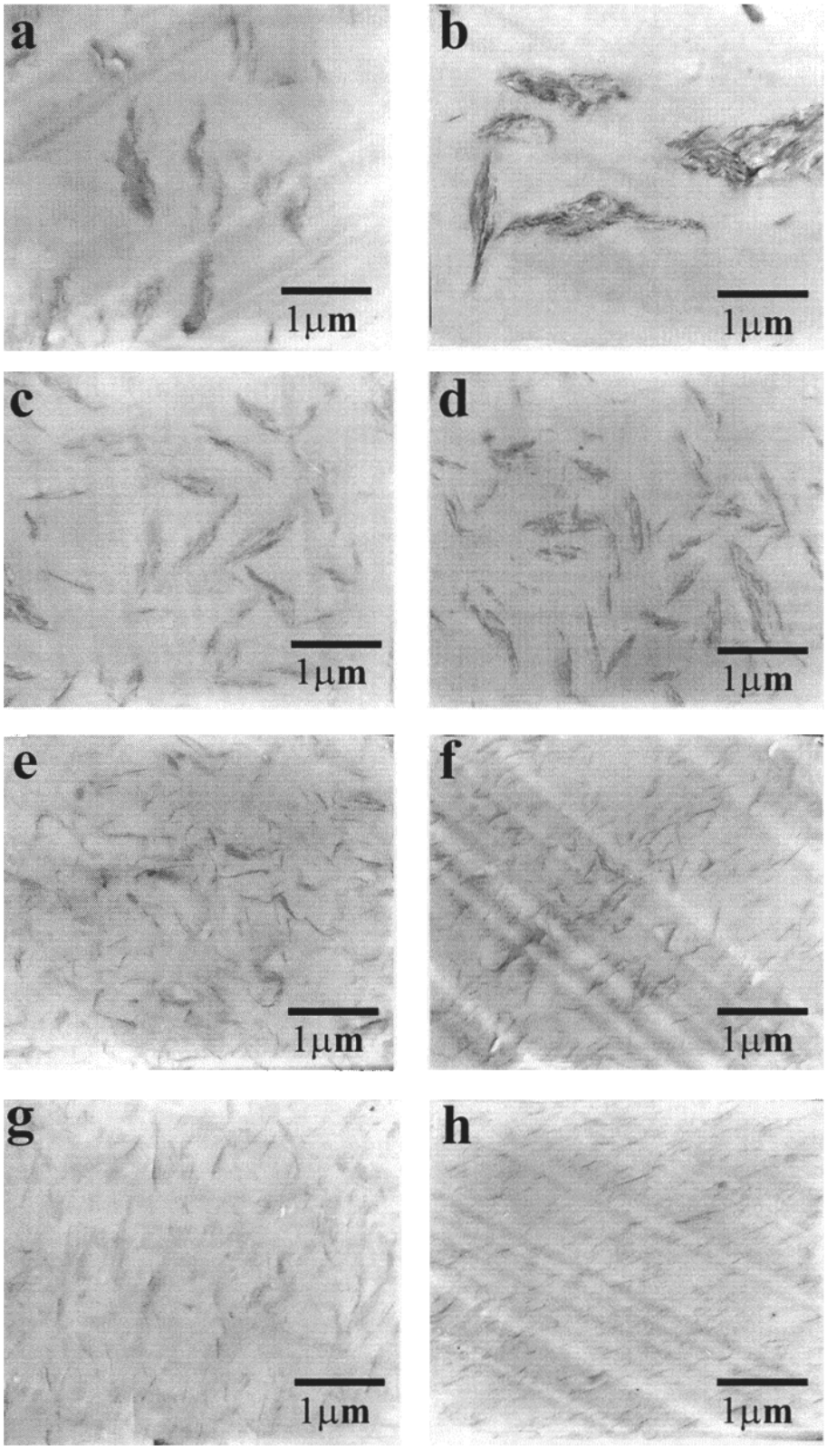


**Figure 4.** TEM micrographs of clay composites: (a) PS/Cloisite® 25A, (b) PS/Cloisite® 30A, (c) SAN5/Cloisite® 25A, (d) SAN5/Cloisite® 30A, (e) SAN25/Cloisite® 25A, (f) SAN25/Cloisite® 30A, (g) SAN41/Cloisite® 25A, (h) SAN41/Cloisite® 30A.

polystyrene can intercalate into the galleries of silicate layers (5). Intercalation of polystyrene was confirmed by the observation of (001) plane peak, though being smaller, around 2.5° ~ 3.0° in the XRD pattern (*see* Figure 3). Thus the intercalation of polystyrene into the galleries of Cloisite® 25A might induce the breaking of clay agglomerates into smaller clay particles.

In the hybrids of SAN other than polystyrene, it can be observed that clay particles or nano-scale building blocks are distributed uniformly and their sizes are strongly dependent on the comonomer content, especially in Cloisite® 30A-dispersed hybrids. Acrylonitrile comonomer incorporated into SAN facilitates the intercalation of copolymers into the galleries of silicate layers modified with an intercalant, i.e. either 2MHTL8 or MT-2EthOH. It might be thought that hydrogen bonding interaction between the nitrile groups of SAN and the hydroxyl groups on silicate layer makes a negative contribution to exchange energy of mixing so that the intercalation of copolymers into the galleries of silicate layers is accelerated. It is, also, expected that the enhanced polarity of SAN due to incorporated acrylonitrile comonomer can destroy the hydrogen bondings of MT-2EthOH in the galleries. This might, also, increases the intercalation rate of SAN into the galleries of silicate layers modified with MT-2EthOH. More importantly, it can be observed from TEM micrographs that the size of clay particle or nano-scale building block in the hybrids using Cloisite® 30A decreases more rapidly as the acrylonitrile content increases rather than that in the hybrids using Cloisite® 25A. Also, nano-scale building block in SAN41/Cloisite® 30A hybrid is the smallest than those in any other matrix polymers, even though being not perfectly delaminated. This might be originated from the greatest intercalation rate of SAN41 into the galleries of Cloisite® 30A due to the enhanced polarity of matrix polymer and the use of intercalant, which has a favorable interaction with matrix polymer.

Flexural properties of the composites were measured to examine the size effect of fillers on reinforcement. Flexural moduli of the hybrids are plotted with those of the corresponding pure matrix polymers in Figure 5(a), and the increase ratios of flexural moduli of the hybrids to those of the corresponding pure polymers are plotted in the upper part of Figure 5(c). The effect of stiffness reinforcement with the addition of clay can be found in any kind of hybrid, but it can be said that the effect of stiffness reinforcement of clay becomes greater as the dispersion of silicate layers in the hybrids becomes better. As discussed in the earlier report (6), the modulus of a hybrid increases as the aspect ratio of dispersed clay particle increases. The aspect ratio of a dispersed clay particle in a hybrid increases as the degree of dispersion of silicate layers increases, assuming the same quantity of loaded inorganics.

Figure 5(b) shows the plot of flexural strengths for the hybrids and pure matrix polymers, and the decrease ratios of flexural strengths of the hybrids to those of the corresponding pure polymers are plotted in the lower part of Figure 5(c). The flexural strengths of hybrids are lower than those of the corresponding pure matrix polymers. The simplest strength prediction models are based on the area reduction of matrix in the presence of particulate fillers. With the addition of particulate fillers, the strength of plastics generally decreases at lower concentration (7,8). When the aspect ratio of clay particle is much smaller, end effect of clay particles becomes progressively more significant because the end effect might reduce the strength of composite (6,9). Because, the strain in end region of clay particle will be less than that in matrix, the shear

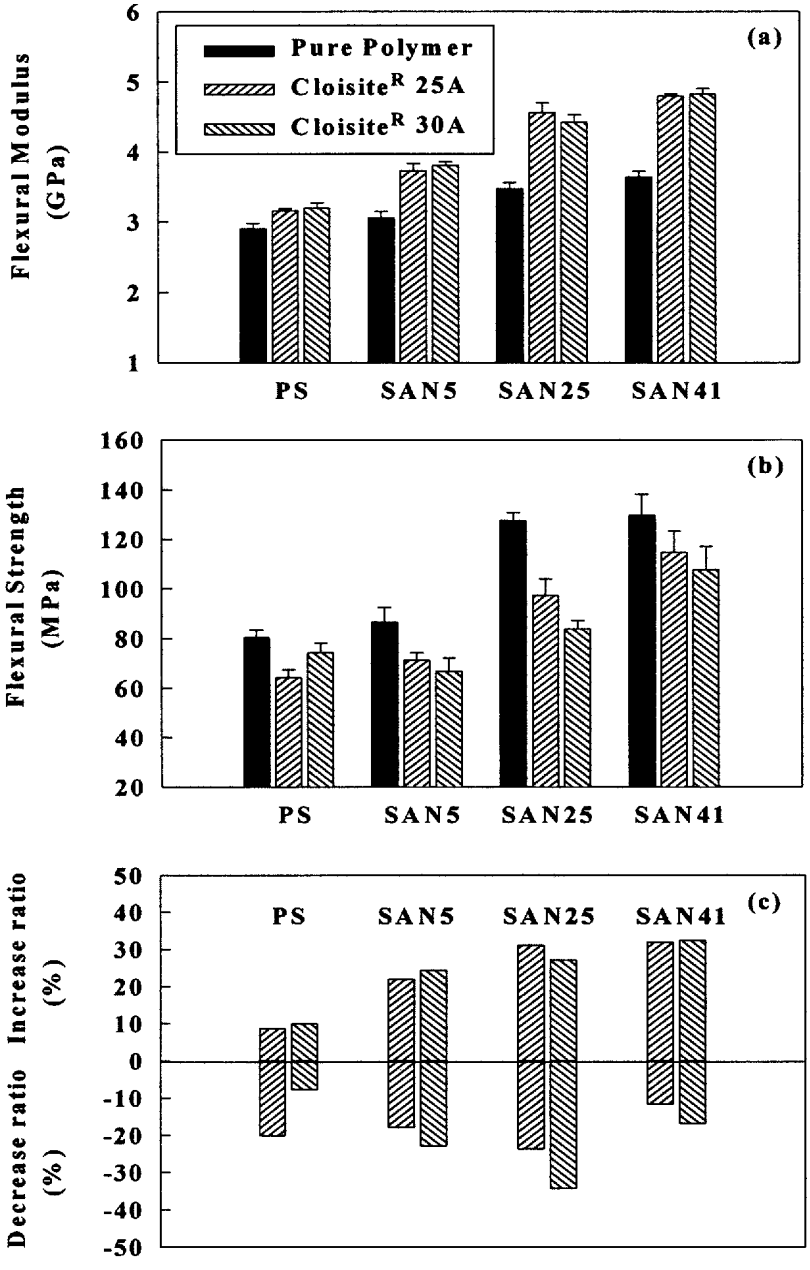


**Figure 5.** Mechanical properties of clay-dispersed composites.

stress of the matrix at interface is larger than the tensile stress in clay particle. The large shear stress of the matrix at the end of clay particle can result in i) shear debonding at the interface, ii) cohesive failure of the matrix, iii) shear yielding of the matrix, depending on the relative failure strengths associated with these processes.

## Conclusions

Clay-dispersed nanocomposites have been prepared by simple melt-mixing of two components, i.e. poly(styrene-*co*-acrylonitrile) copolymers with different contents of acrylonitrile comonomer and two different kinds of organophilic clay (Cloisite® 25A and Cloisite® 30A), with a twin screw extruder. Dispersion behavior of 10-Å-thick

silicate layers of clay in the hybrid was investigated by using an X-ray diffractometer and a transmission electron microscope. Non-hydrogen bonding liquid such as polystyrene does not compatible with Cloisite® 30A treated with methyl tallow bis-2hydroxyethyl ammonium, resulting in no intercalation of polystyrene and remaining of larger clay agglomerates. Meanwhile, the presence of dimethyl hydrogenated-tallow (2-ethylhexyl) ammonium in the galleries of Cloisite® 25A renders the hydrophilic silicate layer more organophilic so that polystyrene can intercalate into the galleries of silicate layers. Acrylonitrile comonomer incorporated into SAN accelerates intercalation of the copolymers into the galleries of silicate layers modified with an intercalant, i.e. either 2MHTL8 or MT-2EthOH, due to hydrogen bonding interaction between the nitrile groups of SAN and the hydroxyl groups on silicate layers, resulting in the enhanced breaking efficiency of clay agglomerates. Moreover, the incorporated polar acrylonitrile comonomer of SAN can destroy the hydrogen bondings of MT-2EthOH in the galleries, which increases the intercalation rate of SAN into the galleries of silicate layers modified with MT-2EthOH. Also, it was observed that the modulus of a hybrid increases as the degree of dispersion of silicate layers increases, assuming the same quantity of loaded inorganics, due to the increased aspect ratio of clay particle.

**Acknowledgements**

This work was supported by the KIST-2000 project (2V00394). The author would like to thank the Southern Clay Products Inc. for providing organophilic clays.

**References**

1. Vaia R.A., Jandt K.D., Kramer E.J., and Giannelis E.P., Macromolecules, 28, 8080 (1995).
2. Vaia R.A., and Gianellis E.P., Macromolecules, 30, 7990 (1997).
3. Hackett E., Manias E., and Gianellis E.P., J. Chem. Phys., 108, 7410 (1998).
4. Barton A.F.M. Ed., Handbook of Solubility Parameters & Other Cohesion Parameters, CRC Press Inc., Boca Raton, 1985, p 41.
5. Vaia R.A., Ishii H., and Gianellis E.P., Chem. Mater., 5, 1694 (1993).
6. Ko M.B., Lim S., Kim J., Choe C.R., Lee M.S. and Ha M.G., Korea Polymer Journal, 7, 310 (1999).
7. Nicolais L., and Nakis M., Polym. Eng. Sci., 11, 194 (1971).
8. Nicolais L., and Masheklar R.A., J. Appl. Polym. Sci., 20, 561 (1976).
9. Holister G.H., and Thomas C. Ed, Fiber Reinforced Materials, Elsevier, London, 1966.